AIP Advances

# Coupled mechanical-oxidation modeling during silicon thermal oxidation process

Yang Zhang, Xian-Cheng Zhang, and Shan-Tung Tu

Citation: AIP Advances **5**, 097105 (2015); doi: 10.1063/1.4930255
View online: http://dx.doi.org/10.1063/1.4930255
View Table of Contents: http://scitation.aip.org/content/aip/journal/adva/5/9?ver=pdfcov
Published by the AIP Publishing



AIP ADVANCES **5**, 097105 (2015)

# Coupled mechanical-oxidation modeling during silicon thermal oxidation process

Yang Zhang, Xian-Cheng Zhang,[a] and Shan-Tung Tu
*Key Laboratory of Pressurized System and Safety, East China University of Science and Technology, Shanghai, 200237, P.R. China*

(Received 10 July 2015; accepted 24 August 2015; published online 2 September 2015)

This work provided an analytical model to solve the coupled mechanical-oxidation problem during the silicon thermal oxidation process. The silicon thermal oxidation behavior under two different mechanical load conditions, i.e., constant strain and uniaxial stress, were considered. The variations of oxide stress and scale thickness along with oxidation time were predicted. During modeling, all the effects of stress accumulation due to growth strain, stress relaxation due to viscous flow and the external load on the scale growth rate were taken into consideration. Results showed that the existence of external loads had an obvious influence on the oxide stress and scale thickness. Generally, tensile stress or strain accelerated the oxidant diffusion process. However, the reaction rate at the $Si/SiO_2$ interface was retarded under uniaxial stress, which was not found in the case of constant strain load.  [http://dx.doi.org/10.1063/1.4930255]

## I. INTRODUCTION

Owing to its great importance in technology,[1–5] the formation of silica layer by silicon thermal oxidation has been extensively studied in the past few years. Differing from the widely accepted parabolic law, the subsequent experimental results indicated that the exponent value was always in the range between 1.0 and 2.0. This phenomenon had not been well explained until Deal and Grove proposed the linear-parabolic model.[1] In their model, the oxidation behavior was influenced not only by the oxidant diffusivity through the scale but also by the reaction rate at the scale/substrate interface.

The silicon components are inevitably subjected to the external mechanical loads during service. Among all situations, two kinds of external mechanical loads are the most common. The first kind is the constant strain load. For example, the mismatch between thermal expansions of silicon substrate and silica layer will induce the thermal stains which remain constant at a given temperature. The other kind is the uniaxial stress load. In terms of loads due to gravity, electricity and others, the stress load is kept constant and the strain of $Si/SiO_2$ system varies along with time. Meanwhile, a lot of previous studies showed that large residual or mechanical stress would be generated during the oxidation process and it had a substantial effect on the oxidation behavior of silicon.[6–9] Researches on the interaction between mechanical stress and oxidation of silicon can be mainly divided into three categories.

The first category was mainly focused on the origin of growth stress in the oxide scale. It was generally believed that the difference of molar volume between the oxide scale and underlying metal, i.e., Pilling and Bedworth ratio, was responsible for the growth stress.[10] Then, Rapp et al.[11,12] proposed a model in which the interfacial defects, such as misfit dislocation and ledges formed during the oxidation process, were considered to play an important role in the generation of growth stress. Recently, Clarke et al.[13,14] proposed a model in which the growth strain was considered to be generated due to the climb of edge dislocations in the oxide. A parameter defined as lateral growth constant was used to describe the ratio of growth strain and scale thickness. Lots of subsequent

[a]Author to whom correspondence should be addressed. Electronic mail: xczhang@ecust.edu.cn

 

analytical models followed Clarke's idea.[15–20] However, in Clark's model, the effect of interfacial defects, such as misfit dislocation, on the growth strain of oxidation layer was not considered.

The second category treated the effect of growth stress on the scale growth rate. Fargeix and Ghibaudo[21,22] proposed a model in which the oxidant diffusivity through the oxide scale, i.e., the parabolic constant, depended on the growth stress. This theory was also followed by Navi et al.,[23] Noma et al.[24] and Delph et al.[25] Meanwhile, Irene et al.[8,26–28] investigated the effect of stress on reaction rate constant and suggested that the reaction rate at the scale/substrate interface was proportional to the magnitude of compressive stress in the scale. Kao et al.[5,29] and Sutardja et al.[30] investigated the two-dimensional thermal oxidation of silicon. Due to the stress effect, the oxide grown on a concave surface was much thinner than that grown on a convex surface. Some other experimental results indicated that mechanical stress can influence both the oxidant diffusivity and the reaction rate.[31,32]

In the third category, the effect of external loads on the oxidation behavior of silicon was considered. Yen et al.[33,34] placed two silicon wafers vertically at one side and put a small slice of quartz across the middle of the wafers to make them bend. However, although the bending deformation of the samples remained constant, the bending moment would diminish with time due to creep deformation. In such a case, the applied load was not the bending stress but the constant strain. The experimental results suggested that tensile strain would lead to the acceleration of the oxidation rate due to the increment of the parabolic constant. Similarly, Tamura et al.[31] carried out the oxidation experiments using three-point bending equipment. The samples were bended and fixed with bolts, leading to the generation of a constant strain load. When the temperature was low, the mechanical stress would affect reaction rate rather than diffusivity. At a higher temperature, its effect on the diffusivity was more obvious. Mihalyi et al.[35] and Lin et al.[36] applied a four-point bending load to the silicon strip. In such a case, the bending moment remained constant during the oxidation process. The results indicated that the compressive stresses tended to retard the growth of the oxide layer while the effect of tensile stress was not clear.

In this paper, an analytical model is proposed to solve the coupled mechanical-oxidation problem in silicon thermal oxidation. The main motivations behind the present work are two-fold. The first is to develop an analytical model to extract the stress and growth rate of the silica layer due to mechanical load. The second is to distinguish the effects of constant strain and uniaxial stress on the growth rate of the silica layer.

## II. FRAMEWORK OF ANALYTICAL MODEL

### A. Growth rate of silica layer

When the diffusion of oxidant is quasistatic,[25] the flux of oxidant throughout the oxide scale remains constant.[25] According to Fick's second law, it can be expressed as

$$\frac{\partial C(x,t)}{\partial t} = \frac{\partial F(x,t)}{\partial x} = \frac{\partial}{\partial x}\left[D_{eff}(x,t)\frac{\partial C(x,t)}{\partial x}\right] = 0 \tag{1}$$

where $C$ is the oxidant concentration, $F$ is the oxidant flux through the silica layer, $D_{eff}$ is the oxidant diffusivity, $x$ is the depth of the silica layer and $t$ is the time. Considering the stress effect on the diffusivity, the effective oxidant diffusivity, $D_{eff}$, due to stress can be expressed as[25]

$$D_{eff} = D_0 \exp\left(\frac{pV_d}{kT}\right) \tag{2}$$

Where $D_0$ is the diffusivity in the stress-free state, $p$ is the hydrostatic normal stress, $V_d$ is the activation volume for diffusion, and $k$ and $T$ are respectively Boltzmann constant and Kelvin temperature. If the biaxial stress in the oxide scale is $\sigma_{ox}$, the magnitude of $p$ should be equal to $2\sigma_{ox}/3$. Considering the oxide scale as a multilayered system, the flux of oxidant through the $i^{th}$ layer, $F^{(i)}$, can be expressed as

$$F^{(i)} = D_{eff}{}^{(i)}\frac{dC}{dx} = \exp\left(\frac{2\sigma_{ox}{}^{(i)}V_d}{3kT}\right) \times \frac{D_0\left(C^{(i)} - C^{(i+1)}\right)}{\delta_{ox}{}^{(i)}} \tag{3}$$

where ${D_{eff}}^{(i)}$ and ${\delta_{ox}}^{(i)}$ are respectively the oxidant diffusivity and thickness of the $i^{th}$ layer, ${\sigma_{ox}}^{(i)}$ is the stress within the $i^{th}$ layer, and $C^{(i)}$ and $C^{(i+1)}$ are respectively the oxidant concentration at the outer and inner boundary of the $i^{th}$ layer. Therefore, if the total number of layers is $K$, the oxide scale thickness, $h_{ox}$, is

$$h_{ox} = \sum_{i=1}^{K} {\delta_{ox}}^{(i)} \tag{4}$$

According to Deal's theory,[1] the flux of oxidant from the gas to the vicinity of the outer surface depends on the oxidant concentration at the outer surface, i.e.,

$$F^{(0)} = m(C^* - C^{(1)}) \tag{5}$$

where $m$ is the gas-phase transport coefficient and $C^*$ is the equilibrium concentration in the gas. Meanwhile, the flux corresponding to the reaction rate at the $Si/SiO_2$ interface can be expressed as[1]

$$F^{(K+1)} = k_i C^{(K+1)} \tag{6}$$

where $k_i$ is the reaction rate constant. In the models of Kao et al.[29] and Sutardja et al.,[30] the effect of stress normal to $Si/SiO_2$ interface, $\sigma_{nn}$, is considered to evaluate the reaction rate constant, i.e.,

$$k_i = k_0 \times \exp\left[\frac{-\sigma_{nn} \times \left(V_{SiO_2} - V_{Si}\right)}{kT}\right] \tag{7}$$

where $k_0$ is the stress free-value of $k_i$, $V_{SiO_2}$ and $V_{Si}$ are respectively the molecular volume of $SiO_2$ and atomic volume of Si. However, under uniaxial mechanical load, the normal stress in the thin $SiO_2$ layer is extremely small. In such a case, $k_i$, is assumed to be independent of oxide stress and remains constant throughout the whole oxidation process. In order to keep the flux at a steady state through the thickness of silica layer, the following equilibrium condition should be satisfied, i.e.,

$$F = F^{(0)} = F^{(1)} = \cdots = F^{(K+1)} \tag{8}$$

Combining Eqs. (3), (5), (6), and (8), the vector of oxidant concentration, $\boldsymbol{C}$, can be obtained, i.e.,

$$\boldsymbol{C} = \boldsymbol{A}^{-1} * \boldsymbol{b} \tag{9}$$

where the matrix $\boldsymbol{A}$ and vector $\boldsymbol{b}$ can be expressed as

$$\boldsymbol{A} = \begin{bmatrix} \left(\frac{{D_{eff}}^{(1)}}{{\delta_{ox}}^{(1)}} + m\right) & -\frac{{D_{eff}}^{(1)}}{{\delta_{ox}}^{(1)}} & 0 & \cdots & \cdots & 0 \\ \frac{{D_{eff}}^{(1)}}{{\delta_{ox}}^{(1)}} & -\left(\frac{{D_{eff}}^{(1)}}{{\delta_{ox}}^{(1)}} + \frac{{D_{eff}}^{(2)}}{{\delta_{ox}}^{(2)}}\right) & \frac{{D_{eff}}^{(2)}}{{\delta_{ox}}^{(2)}} & 0 & \cdots & 0 \\ 0 & \ddots & \ddots & \ddots & \cdots & \vdots \\ \vdots & 0 & \frac{{D_{eff}}^{(i-1)}}{{\delta_{ox}}^{(i-1)}} & -\left(\frac{{D_{eff}}^{(i-1)}}{{\delta_{ox}}^{(i-1)}} + \frac{{D_{eff}}^{(i)}}{{\delta_{ox}}^{(i)}}\right) & \frac{{D_{eff}}^{(i)}}{{\delta_{ox}}^{(i)}} & \vdots \\ 0 & \cdots & \ddots & \ddots & \ddots & 0 \\ 0 & \cdots & \cdots & 0 & \frac{{D_{eff}}^{(K)}}{{\delta_{ox}}^{(K)}} & -\left(\frac{{D_{eff}}^{(K)}}{{\delta_{ox}}^{(K)}} + k_i\right) \end{bmatrix} \tag{10a}$$

$$\boldsymbol{b} = \begin{bmatrix} m\boldsymbol{C}^* \\ 0 \\ \vdots \\ 0 \end{bmatrix} \tag{10b}$$

The solution of Eq. (9) is

$$C^{(i)} = L^{(i)} C^{(K+1)} \tag{11}$$

where

$$L^{(i)} = \begin{cases} \dfrac{D_{eff}^{(i)}}{\delta_{ox}^{(i)}} \times \left( \dfrac{D_{eff}^{(i+1)}}{\delta_{ox}^{(i+1)}} L^{(i+1)} + \dfrac{D_{eff}^{(i)}}{\delta_{ox}^{(i)}} L^{(i+1)} - \dfrac{D_{eff}^{(i+1)}}{\delta_{ox}^{(i+1)}} L^{(i+2)} \right) & i = 1,2,\ldots,K-1 \\ \dfrac{D_{eff}^{(K)} + k_i \delta_{ox}^{(K)}}{D_{eff}^{(K)}} & i = K \\ 1 & i = K+1 \end{cases} \tag{12a}$$

$$C^{(K+1)} = \frac{m\delta_{ox}^{(1)} C^*}{\left(D_{eff}^{(1)} + m\delta_{ox}^{(1)}\right) L^{(1)} - D_{eff}^{(1)} L^{(2)}} \tag{12b}$$

If $N$ is the number of oxidant molecules incorporated into a unit volume of the oxide layer, the scale growth rate equals $F/N$.[1] At the $(K+1)^{th}$ step, the following equation should be satisfied, i.e.,

$$\frac{dh_{ox}}{dt} = \frac{F}{N} = \frac{\delta_{ox}^{(K)}}{\Delta t} \tag{13}$$

where $\Delta t$ is the time step. According to Eq. (13), scale growth rate is a function of multilayer thicknesses and stresses in these layers. The solving method of Eq. (13) will be presented in the following section.

### B. Growth strain within silica layer

In the present model, the total growth strain of silica layer, $\varepsilon_g$, is composed of two kinds of growth strain, $\varepsilon_{g1}$ and $\varepsilon_{g2}$, which are respectively generated at the $Si/SiO_2$ interface and during the scale growth process, i.e.,

$$\varepsilon_g = \varepsilon_{g1} + \varepsilon_{g2} \tag{14}$$

During the oxidation process, some silicon atoms at the $Si/SiO_2$ interface must diffuse away to maintain the misfit dislocation concentration at the interface. If the required atoms diffuse very slowly, the first kind of growth strain, $\varepsilon_{g1}$, would be generated at the interface.[12] Meanwhile, some of these excess silicon atoms flow interstitially into the oxide and react with the diffusing oxidant.[37–39] Due to the fact that the value of $V_{SiO_2}$ is much larger than that of $V_{Si}$, the second kind of growth strain, $\varepsilon_{g2}$, is continuously generated as the silica layer thickening. In atmosphere of dry O2 with 4.5% HCl, the growth stress of thermally grown silica layer on (100) Si substrate increased at initial oxidation stage and then decreased gradually,[6] indicating the existence of $\varepsilon_{g2}$. Since $\varepsilon_{g1}$ remains constant throughout the scale growth process, the growth strain rate, $\dot{\varepsilon}_g$, is equal to $\dot{\varepsilon}_{g2}$. In the present model, $\varepsilon_{g2}$ is assumed to be proportional to the concentration of interstitial silicon atoms, diffusing flux of oxidant and the volume ratio between $SiO_2$ and Si. Thus, the lateral growth constant, $r_{ox}$, can be proposed from the following equation,

$$\dot{\varepsilon}_g = \dot{\varepsilon}_{g2} = r_{ox}\dot{h}_{ox} \tag{15}$$

Equation (15) is similar to that of Clarke's model[13,14] which is widely used to describe the growth strain in the oxidation layer on ceramic material. However, it should be noted that the physical meaning of Clarke's model is different from that of the present model. In Clarke's model, the climb of dislocation is induced by the diffusion of ions in the scale, which contributes to the generation of growth strain within the oxide scale.

### C. Equilibrium condition due to constant strain

At a given externally applied strain, $\varepsilon_0$, the total strain of substrate can be expressed as the sum of elastic strain, $\varepsilon_{e,m}$, and creep strain, $\varepsilon_{c,m}$, i.e.,

$$\varepsilon_0 = \varepsilon_m = \varepsilon_{e,m} + \varepsilon_{c,m} = \frac{1-\upsilon_m}{E_m}\sigma_m + \varepsilon_{c,m} \tag{16}$$

where $E_m$ and $v_m$ respectively represent the elastic modulus and Poisson's ratio of silicon substrate. It is assumed that the creep strain rate of the silicon substrate, $\dot{\varepsilon}_{c,m}$, obeys Norton's power law, namely

$$\dot{\varepsilon}_{c,m} = \mathrm{sgn}(\sigma_m) \cdot A_m \cdot |\sigma_m|^{n_m} \tag{17}$$

where $A_m$ and $n_m$ respectively represent the creep constant and index of silicon, and sgn is the signum function. Keeping the total strain constant and differentiating Eq. (16) with respect to time, the strain rate of the substrate can be expressed as

$$\dot{\varepsilon}_m = \frac{1 - v_m}{E_m}\dot{\sigma}_m + \mathrm{sgn}(\sigma_m) \cdot A_m \cdot |\sigma_m|^{n_m} = \dot{\varepsilon}_0 = 0 \tag{18}$$

Hence, the elastic stress of the substrate, $\sigma_m$, can be expressed as

$$\sigma_m = \left\{(-n_m + 1) \times \left[-\frac{A_m(1 - v_m)}{E_m}t\right] + \left(\frac{\varepsilon_0 E_m}{1 - v_m}\right)^{-n_m+1}\right\}^{\frac{1}{-n_m+1}} \quad \text{if } \varepsilon_0 \geq 0 \tag{19a}$$

$$\sigma_m = -\left\{(-n_m + 1) \times \left[-\frac{A_m(1 - v_m)}{E_m}t\right] + \left(-\frac{\varepsilon_0 E_m}{1 - v_m}\right)^{-n_m+1}\right\}^{\frac{1}{-n_m+1}} \quad \text{if } \varepsilon_0 < 0 \tag{19b}$$

The total strain of $i^{\text{th}}$ silica layer, ${\varepsilon_{ox}}^{(i)}$, can be expressed as the sum of elastic strain, ${\varepsilon_{e,ox}}^{(i)}$, viscous strain, ${\varepsilon_v}^{(i)}$, growth strain, ${\varepsilon_g}^{(i)}$, and the strain due to the change of silica concentration at the interface, ${\varepsilon_n}^{(i)}$, i.e.,

$$\varepsilon_0 = {\varepsilon_{ox}}^{(i)} = \frac{1 - v_{ox}}{E_{ox}}{\sigma_{ox}}^{(i)} + {\varepsilon_v}^{(i)} + {\varepsilon_g}^{(i)} + {\varepsilon_n}^{(i)} \tag{20}$$

where $E_{ox}$ and $v_{ox}$ respectively represent the elastic modulus and Poisson's ratio of silica layer. As a result of the creep strain of the substrate, the silicon atom number varies along with time. Keeping the volume ratio of silica to silicon constant, the silica concentration at the interface is proportional to that of silicon there. For every silica layer, ${\varepsilon_n}^{(i)}$ remains unchanged along with time. Detailed expression of ${\varepsilon_n}^{(i)}$ can be seen in Section II E. The viscous strain rate, ${\dot{\varepsilon}_v}^{(i)}$, can be expressed as[21,22]

$${\dot{\varepsilon}_v}^{(i)} = \frac{{\sigma_{ox}}^{(i)}}{\tau} \times \frac{1 - v_{ox}}{E_{ox}} \tag{21}$$

where $\tau$ is the Maxwellian relaxation time, which is the ratio of viscosity, $\eta$, and shear modulus, $\mu$. The following equilibrium equation can be obtained through differentiating Eq. (20) with respect to time,

$${\dot{\varepsilon}_{ox}}^{(i)} = \frac{1 - v_{ox}}{E_{ox}}{\dot{\sigma}_{ox}}^{(i)} + \frac{{\sigma_{ox}}^{(i)}}{\tau} \times \frac{1 - v_{ox}}{E_{ox}} + r_{ox}\dot{h}_{ox} = 0 \tag{22}$$

At the $i^{th}$ step, the oxidation time is $(i + 1)\Delta t$, the $i^{th}$ scale layer appears. At this time, the creep strain of substrate is $\varepsilon_{c,m}|_{t=(i+1)\Delta t}$. Due to the constant strain load, the total strain of the $i^{th}$ scale layer is $\varepsilon_0$. In such a case, the initial elastic strain of the $i^{th}$ scale layer can be expressed as

$${\varepsilon_{ini}}^{(i)} \approx \varepsilon_0 + \varepsilon_{g1} - \varepsilon_{c,m}|_{t=(i+1)\Delta t} \tag{23}$$

Equation (23) will be demonstrated in the section II E. Since that the total strain of silicon is the sum of creep strain and elastic strain, at the time of $(i + 1)\Delta t$, the following equation can be obtained

$${\sigma_{ini}}^{(i)} = \frac{E_{ox}}{1 - v_{ox}}\left(\frac{1 - v_m}{E_m}\sigma_m\Big|_{t=(i+1)\Delta t} + \varepsilon_{g1}\right) \tag{24}$$

where the expression of $\sigma_m$ has been given in Eq. (19). Then the variations of oxide stress and scale thickness along with time can be obtained by combining Eqs. (10)–(12), (19), (22) and (24).

### D. Equilibrium condition due to uniaxial stress

For the case of constant uniaxial stress, besides the strain compatibility at the interface, the stress equilibrium should be taken into consideration. If the external uniaxial stress is $\sigma_0$, the stress equilibrium can be expressed as

$$\int_0^{h_{ox}(t)} \sigma_{ox}(x,t)\,dt + \int_{h_{ox}(t)}^{h_{ox}(t)+h_m/2} \sigma_m dx = \left(h_{ox} + \frac{h_m}{2}\right)\sigma_0 \tag{25}$$

where $\sigma_m$ is stress in the substrate, and $h_m$ is the thickness of the substrate. Generally, the thickness of oxide layer was much lower than that of the underlying substrate. Hence, the substrate thickness is assumed to remain constant during oxidation process. Assuming a uniform distribution of $\sigma_m$, the following equation can be obtained by differentiating Eq. (25) with respect to time,

$$\frac{dh_{ox}}{dt}\sigma_{ox}(x,t)\Big|_{x=h_{ox}} + \int_0^{h_{ox}} \frac{\partial \sigma_{ox}(x,t)}{\partial t}dx + \frac{d\sigma_m}{dt}\cdot\frac{h_m}{2} = \frac{dh_{ox}}{dt}\sigma_0 \tag{26}$$

Replacing integral operation with series operation at the $(K+1)^{th}$ step, Eqs. (25) and (26) can be rewritten as

$$\sigma_m = \frac{2\sigma_0}{h_m}\left(\sum_{i=1}^{K} {\delta_{ox}}^{(i)} + \frac{h_m}{2}\right) - \frac{2}{h_m}\sum_{i=1}^{K} {\sigma_{ox}}^{(i)}{\delta_{ox}}^{(i)} \tag{27a}$$

$$\dot{\sigma}_m = \frac{2{\delta_{ox}}^{(K)}}{h_m \Delta t}\left(\sigma_0 - {\sigma_{ox}}^{(K)}\right) - \frac{2}{h_m}\sum_{i=1}^{K} {\sigma_{ox}}^{(i)}{\delta_{ox}}^{(i)} \tag{27b}$$

Based on the strain equilibrium condition in the $i^{th}$ scale, the following equation should be satisfied,

$${\varepsilon_{ox}}^{(i)} = \varepsilon_m = \varepsilon \tag{28}$$

where $\varepsilon$ is the total strain of the system. Differentiating it with respect to time, it can be expressed as

$$\frac{1-\upsilon_{ox}}{E_{ox}}{\dot{\sigma}_{ox}}^{(i)} + \frac{{\sigma_{ox}}^{(i)}}{\tau} + r_{ox}\dot{h}_{ox} = \frac{1-\upsilon_m}{E_m}\dot{\sigma}_m + A_m|\sigma_m|^{n_m}\mathrm{sgn}\,(\sigma_m) \tag{29}$$

Substituting Eq. (27) into Eq. (29), the vector of stress rate of the multilayered oxide, $\dot{\boldsymbol{\sigma}}_{ox}$, can be expressed

$$\dot{\boldsymbol{\sigma}}_{ox} = \boldsymbol{B}^{-1} * \boldsymbol{y} \tag{30}$$

where the matrix $\boldsymbol{B}$ is

$$B_{i,j} = \begin{cases} \dfrac{2E_m{\delta_{ox}}^{(i)}}{(1-\upsilon_m)h_m} - \dfrac{E_{ox}}{1-\upsilon_{ox}} & i = j \\ \dfrac{2E_m{\delta_{ox}}^{(i)}}{(1-\upsilon_m)h_m} & i \neq j \end{cases} \tag{31}$$

And the vector $\boldsymbol{y}$ can be expressed as

$$\begin{aligned} y_i = &-A_m\left|\frac{2\sigma_0}{h_m}\left(\sum_{i=1}^{K}{\delta_{ox}}^{(i)} + \frac{h_m}{2}\right) - \frac{2}{h_m}\sum_{i=1}^{K}{\sigma_{ox}}^{(i)}{\delta_{ox}}^{(i)}\right| \\ &\times \mathrm{sgn}\left[\frac{2\sigma_0}{h_m}\left(\sum_{i=1}^{K}{\delta_{ox}}^{(i)} + \frac{h_m}{2}\right) - \frac{2}{h_m}\sum_{i=1}^{K}{\sigma_{ox}}^{(i)}{\delta_{ox}}^{(i)}\right] \\ &+ \left[r_{ox} - \frac{2E_m\left(\sigma_0 - {\sigma_{ox}}^{(K)}\right)}{h_m(1-\upsilon_m)}\right]\times\frac{{\delta_{ox}}^{(K)}}{\Delta t} + \frac{{\sigma_{ox}}^{(K)}}{\tau} \end{aligned} \tag{32}$$

When the $i^{th}$ oxide layer appears on a deformed substrate, its initial elastic stress, can be expressed as

$$\sigma_{ini}^{(i)} = \frac{E_{ox}}{1-v_{ox}}\left[(1+\varepsilon)-(1+\varepsilon_{c,m})(1-\varepsilon_{g1})\right] \approx \frac{E_{ox}}{1-v_{ox}}\left(\frac{1-v_m}{E_m}\sigma_m+\varepsilon_{g1}\right) \tag{33}$$

The variations of oxide stress and scale thickness along with time can be obtained by combining Eqs. (11)–(13), (29) and (31)–(33).

### E. Initial elastic strain of each silica layer

Being applied of elastic stress, the lattice of silicon will be changed. And the change of lattice distance should be proportional to elastic strain, namely

$$\varepsilon_{e,m} = \frac{d-d_0}{d_0} \tag{34}$$

where $d$ and $d_0$ are respectively the lattice distances at the stressed and stress-free states. The total strain can be expressed as

$$\varepsilon_m = \frac{n\times d - n_0\times d_0}{n_0\times d_0} \tag{35}$$

where $n$ and $n_0$ are respectively the quantities of silicon atoms at a unit length. As mentioned in Eq. (16), the total strain of silicon is the sum of elastic strain and creep strain. Combining Eqs. (16), (34) and (35), when the elastic strain of substrate is much smaller than 1, the creep stain of the substrate can be expressed as

$$\varepsilon_{c,m} = \frac{n-n_0}{n_0}(1+\varepsilon_{e,m}) \approx \frac{n-n_0}{n_0} \tag{36}$$

As seen in Fig. 1, the deformation of silicon substrate is related to both lattice expansion and change of the number of atoms. At first, the elastic stress leads to the lattice expansion. After that, creep deformation due to dislocation climb takes place. During this process, the total deformation is kept constant. The increase of atom number is accompanied by the lattice reduction, and then the elastic stress is relaxed gradually. According to Eq. (36), the creep strain is proportional to the increase of atom quantity at the unit length.

Generally, the first kind of growth stress, $\varepsilon_{g1}$, is kept constant, value of which is depending on the silicon atom diffusing rate and misfit dislocation concentration. Meanwhile, the concentration ratio of silica to silicon is kept constant at the interface, since the volume ratio of silica to silicon remains as large as 2.26. Due to creep deformation, the silicon atoms number at a unit length changes from $n_0$ to $n$, and the silica concentration increases to its $n_0/n$ times. Thus, for the new formed silica layer, the strain due to silica concentration change, $\varepsilon_n$, is same to the creep strain of the substrate, $\varepsilon_c$, at the temporary oxidation time. In such a case, without the constraint at the $Si/SiO_2$ interface, the lateral length of the oxide layer will extend to its $(1-\varepsilon_{g1})n/n_0$ times. The total strain of the $Si/SiO_2$ system remains as large as $\varepsilon$ when the external load is applied. At the initial state, the second growth strain and the viscous strain within the silica layer don't exist, and then the following equation can be obtained

$$\varepsilon_{e,ox} = (1+\varepsilon)-(1-\varepsilon_{g1})\frac{n}{n_0} = (1+\varepsilon)-(1-\varepsilon_{g1})(1+\varepsilon_{c,m}) \approx \varepsilon+\varepsilon_{g1}-\varepsilon_{c,m} \tag{37}$$

Equation (37) can be used to calculate the initial elastic strain of each silica layer, since there is no viscous strain in the new formed layer.

## III. RESULTS AND DISCUSSION

### A. Material parameters for modeling

In the following sections, the (111) Si will be used to illustrate the effect of different types of external loads on the scale stress and scale growth rate. The oxidation temperature is kept to

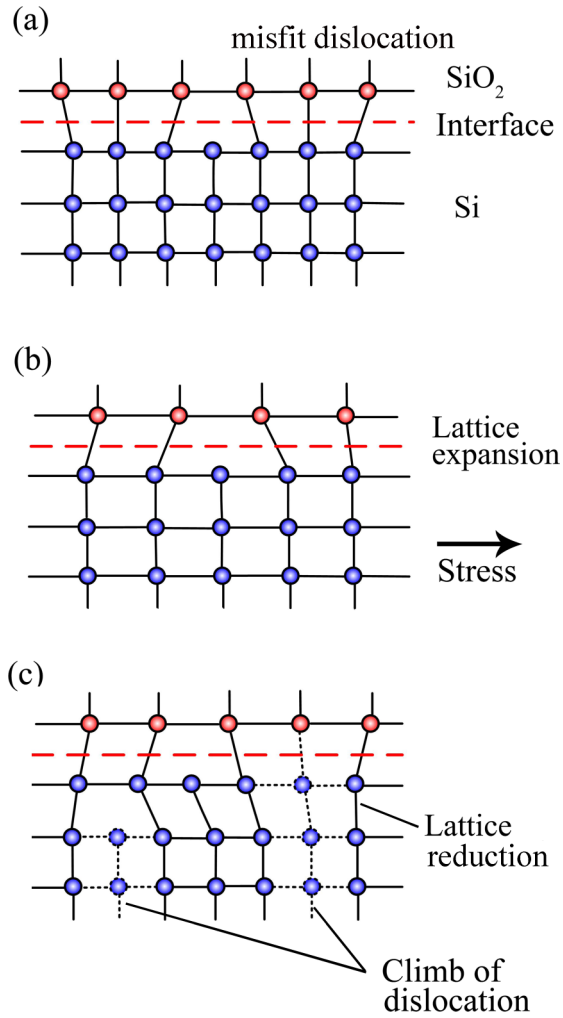


FIG. 1. Schematically showing the deformation processes of silica/silicon system due to external stress, (a) misfit dislocations exist at interface, (b) expansion of silicon lattice due to tensile stress, and (c) stress relaxation and lattice reduction due to climb of dislocation in the substrate.

be 800 °C. Most parameters were exacted from the work of Deal and Grove[1] by Delph et al.[25], i.e., $D_0 = 1.8 \times 10^{-10}$ m$^2 \cdot$ h$^{-1}$, $h = 100$ m $\cdot$ h$^{-1}$, $k_i = 2.3 \times 10^{-3}$ m $\cdot$ h$^{-1}$, $C^* = 5.2 \times 10^{22}$ mol $\cdot$ m$^{-3}$, $N = 2.25 \times 10^{28}$ m$^3$, $E_{ox} = 80$ GPa, $\upsilon_{ox} = 0.28$, $E_m = 130$ GPa, $\upsilon_m = 0.19$ and $h_m = 0.371$ mm. The creep constant and index of silicon substrate at the stationary stage are set to be $1.68 \times 10^{-11}$ MPa$^{-n} \cdot$ s$^{-1}$ and 3.3.[40] At the temperature range from 700 to 1200 °C, $\log \tau$ is a linear function of $1/T$, namely[22]

$$\tau = \tau_0 \exp\left(-\frac{A}{T}\right) \tag{38}$$

where $A$ is the linear coefficient and $\tau_0$ is a constant. The experimental data provided by Fargeix et al.[22] and fitting result are both presented in Fig. 2. The predicted Maxwellian relaxation time at 800 °C is 126250 s.

The value of activation volume, $V_d$, and lateral growth constant, $r_{ox}$, cannot be found from the available literature and they are obtained by the fitting method in this paper. As mentioned above, the growth stress has an important effect on the oxidant diffusivity. At the temperature of 780 °C, the diffusivity of oxidant increased to its 6.5 times when the initial growth stress disappears,[21] meaning the product of initial growth stress and activation volume is kept to be $-4.08 \times 10^{-20}$ J according to Eq. (2). Thus, the value of $V_d$ is set to be $9.0067 \times 10^{-29}$ m$^3$, since initial growth stress

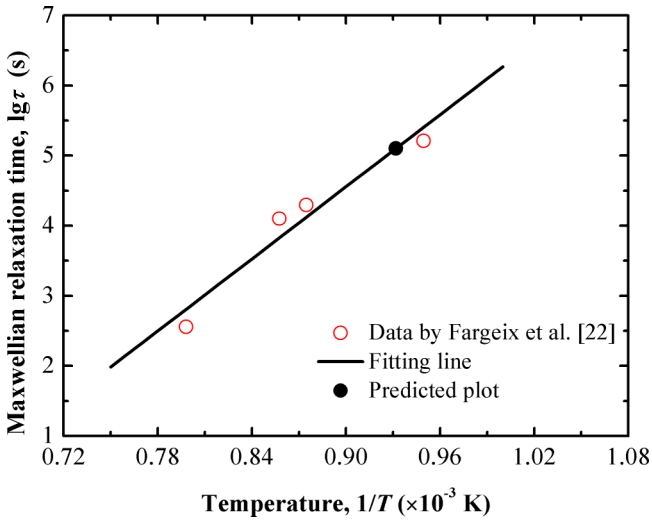


FIG. 2. Variation of Maxwellian relaxation time along with time. At 800 °C, the Maxwellian relaxation time is predicted to be 126250 s.

is determined to be −450 MPa.[8] Then only $r_{ox}$ need to be determined by the fitting approach. The predicted stress within the surface silica layer and the experimental data obtained by Irene et al.[8] are both presented in Fig. 3. During calculation, the time step is set as 5 s. No external load was applied during the oxidation process.[8] The values of $r_{ox}$ can be determined through calculating the minimized quadratic difference sum between the experimental and predicted results. When $r_{ox}$ is 5625 $m^{-1}$, the predicted results agree well with the experimental data.

### B. Effect of constant strain on oxide stress and scale thickness

During calculation, the time step is set as 0.2 s. Constant strains with values of $\pm 2.7 \times 10^{-3}$ are used. It is clear that the applied strain has an obvious influence on the average oxide stress within the oxide scale, especially at the early stage in the oxidation process, as seen in Fig. 4(a). Negative strain enlarges the compressive stress while positive strain reduces it. Due to inelastic strain of both silicon and silica, the induced stress will be relieved gradually. However, the silicon creep strain is supposed to be the dominant reason, since its value is much higher than that of the silica viscous strain at such a temperature.

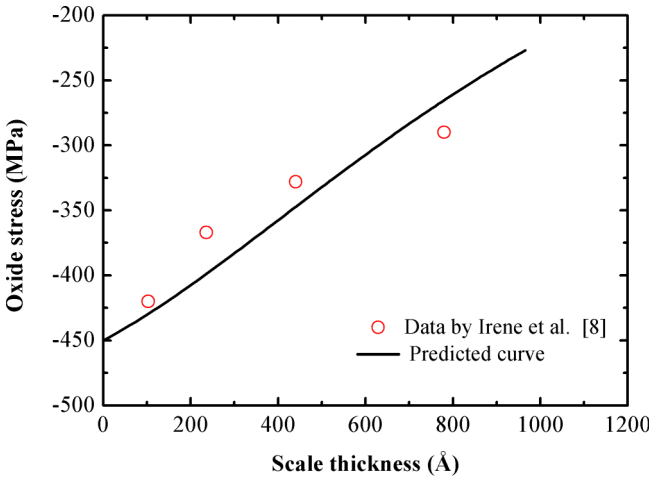


FIG. 3. Variation of growth stress along with time. When $r_{ox}$ is 5625 $m^{-1}$, the predicted result agrees well with experimental data.

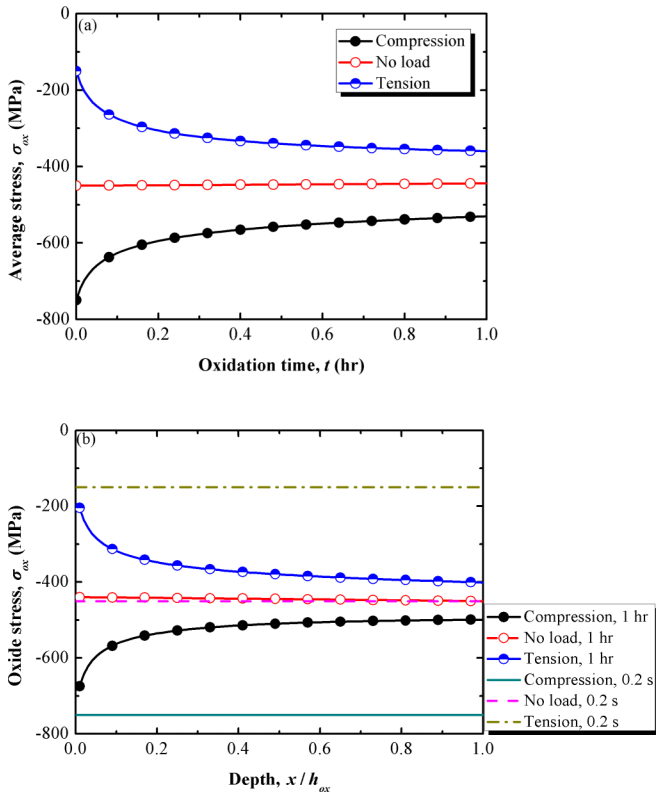


FIG. 4. Variations of oxide stress under constant strain load of $\pm 2.7 \times 10^{-3}$, along with (a) time and (b) scale depth.

Stress distribution along with the scale depth is shown in Fig. 4(b). As mentioned above, when new oxide layer appears on a deformed substrate, its initial elastic stress depends on the creep strain of silicon at that point. During the simulation, the stress state after the first step, i.e., oxidation time of 0.2 s, is regarded as the initial state. At the initial state, the stress was uniformly distributed along with the scale. After 1 hr, the compressive stress decreases due to compressive load and increases due to tensile load. A certain amount of induced stress has been relieved by the creep strain of silicon substrate. As a result, the absolute value of stress gradient decreases along with the scale depth. Hence, the effect of constant strain load on the outer silica layers is more obvious than the inner layers.

Figure 5(a) shows the effect of constant strain load on the thickness of silica scale, $h_{ox}$. Detailed information of parameters used in the calculation is presented in Table I. The values of strain are respectively set to be $\pm 9 \times 10^{-4}$ and the oxidation temperature is kept to be 800 °C. The applied strains of $-9 \times 10^{-4}$ and $+9 \times 10^{-4}$ respectively induce initial elastic stresses of −100 MPa and +100 MPa. By comparing with the scale thickness without applied strain, the scale thicknesses respectively decreases by 8.42% and increases by 7.53% after one hr.

Experimental results by Tamura et al.[31] are also presented in Fig. 5(a). Constant strain loads were applied to the samples and the induced initial elastic stress were also ±100 MPa. By comparing with the scale thickness without applied strain, the scale thicknesses respectively decreases by 10.58% and increases by 7.98% after one hr. From Fig. 5(a), the thickness of oxide sale on the (001) Si substrate used in experiment by Tamura et al.[31] is generally larger than that on the (111) Si used in the present calculation at a given oxide time. This phenomenon is due to the fact that the silica layer growth rate is strongly dependent on the orientation of silicon.[27] However, similar trends can be found in both experimental and predicted results, i.e., positive applied strains accelerate the oxidation rate while negative ones retard it. According to Eq. (2), although the orientation of silicon is different, the increasing percent (or decreasing percent) of diffusivity due to applied stress should be the same if the value of applied strain is given. This result can be verified in Figs. 5(a). Fig. 5(b) shows the

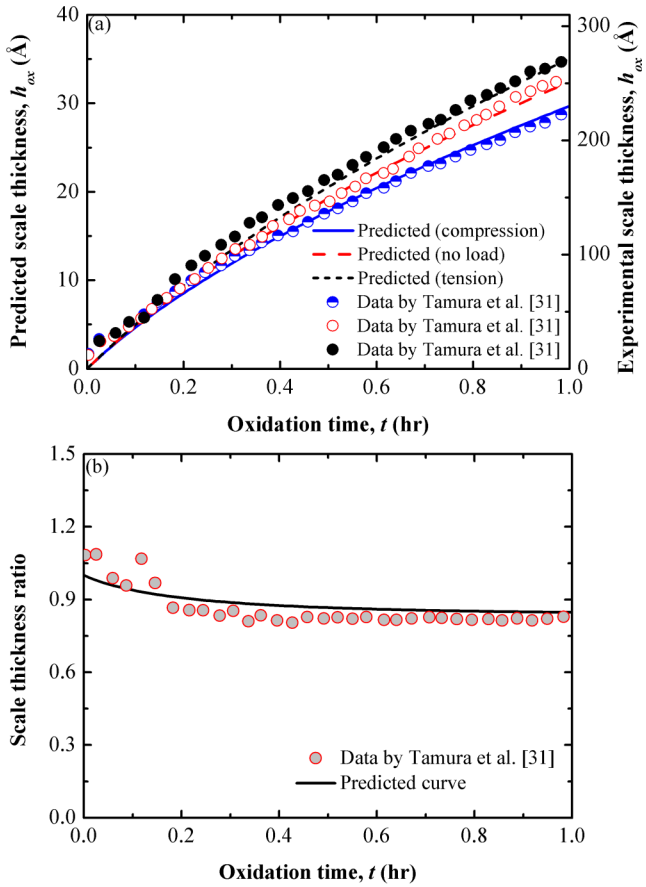


FIG. 5. (a) Variation of scale thickness along with oxidation time: prediction results using (111) Si substrate and experimental results using (001) Si substrate;[31] (b) ratio of scale thickness under compressive load to that under tensile load: prediction results using (111) Si substrate and experimental results using (001) Si substrate.[31]

variation of the ratio of scale thickness under compressive load to that under tensile load along with time. The scale thickness without loads is not involved in the comparison, since its values of horizontal axis are different from those under loading conditions, as seen the experimental data shown in Fig. 5(a). The predicted curve agrees well with the experimental data provided by Tamura et al.[31] Moreover, experimental results by Hwu et al.[33,34] and Kao et al.[7,29] also indicated that tensile loads accelerated the silicon oxidation process while compressive load retarded it. However, since the aim of their experiments was to investigate the non-uniform oxidation behavior of two-dimensional silicon specimens, it is hard to compare their results and the present prediction results directly.

TABLE I. Parameters used in calculation.[8,21,22,25,40]

| Parameters | Value | Parameters | Value |
|---|---|---|---|
| $D_0$ ($m^2 \cdot h^{-1}$) | $1.8\times10^{-10}$ | $E_m$ (GPa) | 130 |
| $h$ ($m \cdot h^{-1}$) | 100 | $v_m$ | 0.19 |
| $k_i$ ($m \cdot h^{-1}$) | $2.3\times10^{-3}$ | $E_{ox}$ (GPa) | 80 |
| $C^*$ ($mol \cdot m^{-3}$) | $5.2\times10^{22}$ | $v_{ox}$ | 0.28 |
| $N$ ($m^3$) | $2.25\times10^{28}$ | $A_m$ (MPa-$^n \cdot s^{-1}$) | $1.68\times10^{-11}$ |
| $V_d$ ($m^3$) | $9.0067\times10^{-29}$ | $n_m$ | 3.3 |
| $r_{ox}$($m^{-1}$) | 5625 | $\tau$ (s) | 126250 |
| $\varepsilon_{g1}$ | $4\times10^{-3}$ | $h_m$ (mm) | 0.371 |
| $T$ (K) | 1073.15 | $\Delta t$ (s) | 0.2 |

### C. Effect of uniaxial stress on oxide stress and scale thickness

In this section, the effect of constant uniaxial stress, $\sigma_0$, on the oxide stress and scale thickness is discussed. The uniaxial stresses with the values of ±15 MPa are applied to the $Si/SiO_2$ system. The variation of average stress along with oxidation time is shown in Fig. 6(a). The applied compressive stress and tensile stress will respectively lead to the increment and decrement of average stress in the oxidation layer. The strain rate of the $Si/SiO_2$ system is non-zero when the external stress is applied. For the silicon substrate, the strain mainly comes from the creep strain. While for the silica layer, its viscous strain is extremely small and the silica layer is nearly elastic. Since the silica scale thickness is much lower than that of the substrate, the strain rate of the system is nearly equal to the creep strain rate of the silicon substrate. Hence, when the uniaxial stress is kept constant, the creep strain rate of the silicon substrate remains nearly unchanged, leading to that the stress in the silica layer increases nearly linearly along with the oxidation time. Stress distribution in the silica layer in the depth direction is shown in Fig. 6(b). At the initial state, i.e., 1 s, the stress was uniformly distributed along with the scale. After 1 hr, the compressive stress value is increased by applied compressive stress and decreased by tensile stress. Absolute value of stress gradient keeps almost constant along with the scale depth.

Figure 7(a) shows the experimental results provided by Lin et al.[36] The uniaxial stresses with the values of ±15 MPa are applied to the $Si/SiO_2$ system. The parameters and their values in Table I are also used in the calculation. The results indicate that both tensile and compressive stress load have a retarding effect on the scale growth rate. This is different from lots of experimental results in which tensile strain loads have a promoting effect.[5,31,33,34] As seen in Fig. 7(a), scale thickness under tensile stress load is still generally higher than that under compressive load, indicating that the oxidant diffusion process is actually accelerated by tensile loads. However, the reduction of the reaction rate, $k_i$, has a more obvious effect than the increase of diffusivity and plays the leading role. It is well known that the density of broken Si-Si bonds at the $Si/SiO_2$ interface is the controlling factor of reaction rate,

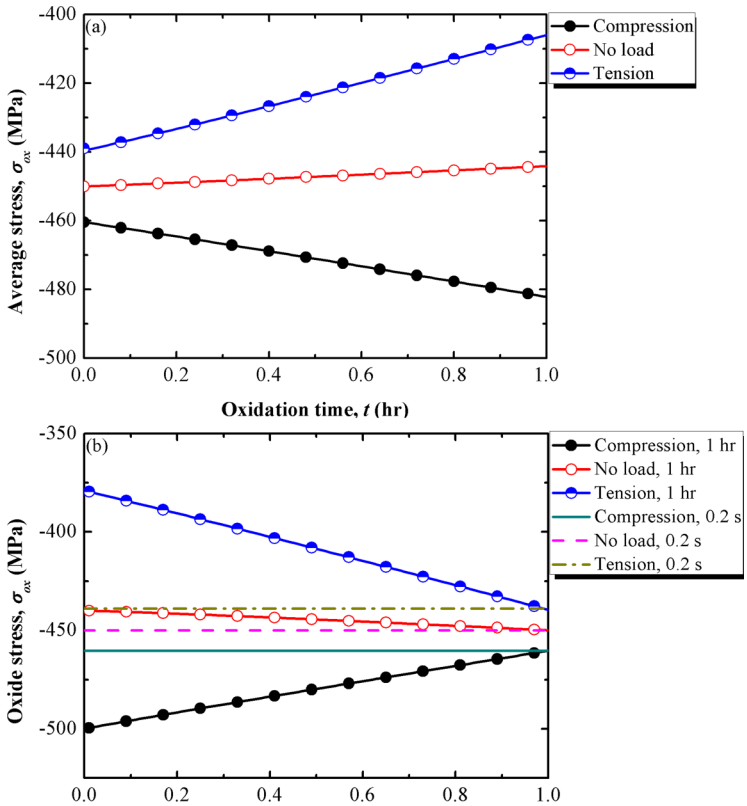


FIG. 6. Variations of oxide stress under constant stress load of ±15 MPa along with (a) time, and (b) along scale depth.

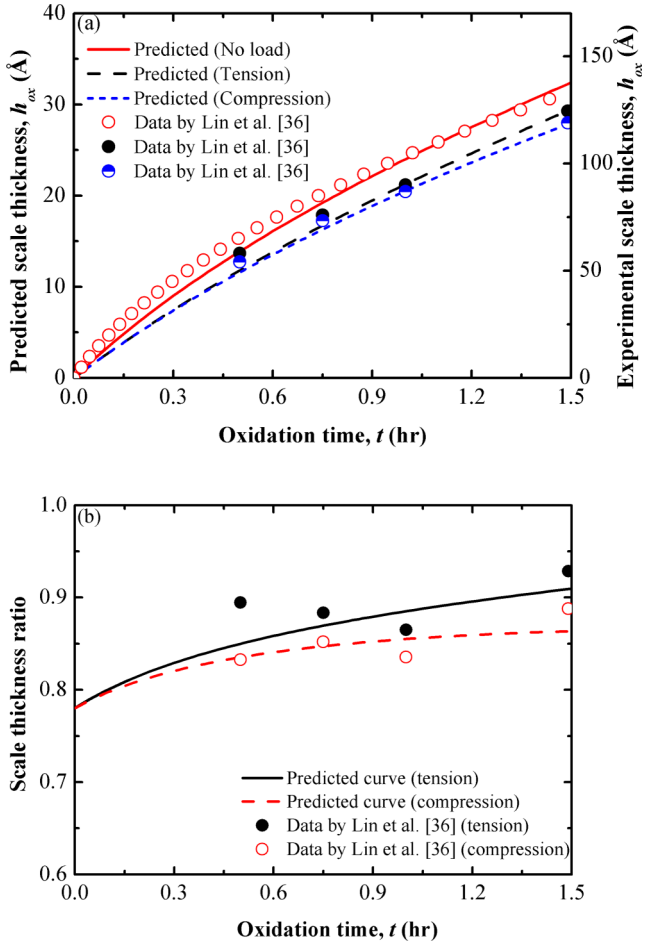


FIG. 7. (a) Variation of scale thickness along with oxidation time: experimental data using (100) Si substrate 36 and predicted results using (111) Si substrate; (b) ratio of scale thickness under unxial loads to that without loads: experimental data using (100) Si substrate[36] and predicted results using (111) Si substrate.

especially at the initial oxidation stage.[38,41] At the interface, silica and silicon are connected by Si-O bonds. The unmatched crystal lattices leave a network of extra half-plane segments on the Si side with associated dangling bonds there.[38] Besides of the misfit dislocation, severe deformation or even distortion of silicon lattice occur near the $Si/SiO_2$ interface to relieve the oxide stress and keep the coherence there. It has been observed that the uppermost one or two layers of silicon atoms beneath the silica scale were displaced up to about 0.015 nm (6.5%) from their lattice positions.[42] As mentioned above, the strains in the silica layer and silicon substrate are respectively due to elastic deformation and creep deformation. In such a case, the lattice of the silica scale is not obviously altered while the number of silicon atoms is changed, leading to the server deformation of the silicon lattice near the $Si/SiO_2$ interface. Thus, the interface becomes an extremely vulnerable region, especially when the strain rate of the system is not zero due to external stress. Our hypothesis is that the sever deformation of the silicon lattice at the interface can cause the break of some amount of the Si-O bond. At the same time, the Si-Si bonds will be formed between the dangling silicon bonds. As a result, the concentration of broken Si-Si bonds at the interface is decreased, leading to the reduction of reaction rate. Hence, a correction factor should be added to $k_i$. However, how to evaluate this factor is still unclear and more researches are still needed. When this factor is assumed to be 0.78, the prediction results agree well with the experimental results by Lin et al.,[36] as shown in Fig. 7(a). The thickness of oxide sale on the (100) Si substrate used in experiment by Lin et al. is generally larger than that on the (111) Si used in the present calculation at a given oxide time. This phenomenon is due to the fact that the silica layer growth rate is strongly dependent on the orientation of silicon.[27]

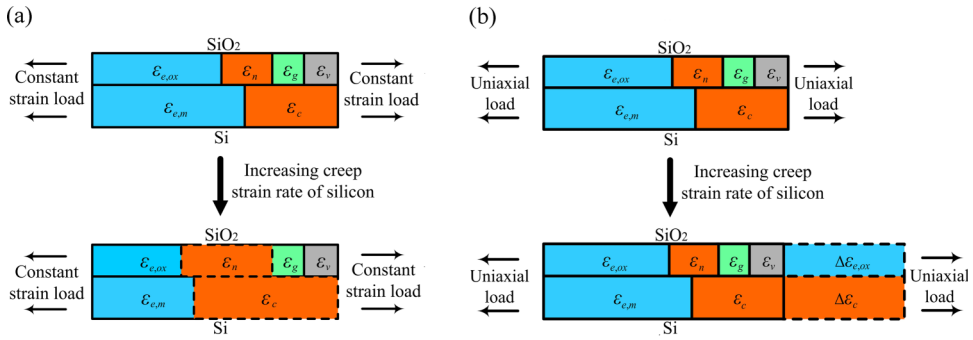


FIG. 8. Schematically showing the opposite effects of (a) constant strain load, and (b) uniaxial stress load on the oxide stress.

Fig. 7(b) shows the ratio of scale thickness under uniaxial stress loads to that without loads. The predicted curve agrees well with the experimental data. A confusing phenomenon in the experiment of Lin et al.[36] is that uniaxial stress of 10 MPa has an even stronger effect than that of 15 MPa, which is still need to be verified. In contrast, other experimental results[5,33,34] indicate that a heavier load leads to a stronger effect.

### D. Effect of temperature

The temperature has two-side effects on the oxide stress level and the scale thickness. Firstly, according to Eq. (2), the oxidant diffusivity is related to temperature. Keeping the oxide stress constant, the effect of stress on oxidation rate is enhanced with decreasing the temperature. Secondly, the creep parameters of silicon substrate strongly depend on the temperature. Creep deformation increases with increasing the temperature. However, the effects of creep deformation on the oxidation behavior of silicon with strain and stress loads are opposite. As seen in Fig. 8(a), for the case of constant strain load, the total strain of the $Si/SiO_2$ remains constant. According to Eq. (37), a larger creep strain of the silicon substrate means a faster stress relaxation process and smaller induced stress. Then according to Eq. (2), the effect of constant strain load on the scale growth rate is weakened. In contrary, for the case of constant stress load, the total strain of the $Si/SiO_2$ is enlarged, as seen Fig. 8(b). A larger silicon creep strain means a larger elastic strain and a larger induced stress within the silica layer. As a result, the effect of load on the scale growth rate is enhanced.

## IV. CONCLUDING REMARKS

The following conclusions were drawn from this work:

1. An analytical model was developed to predict the variations of oxide stress and scale thickness during silicon oxidation. In this model, the synergistic effects of externally mechanical loads, growth strain, elastic strain and inelastic strain were taken into consideration.
2. The effects of two different external loads, i.e., constant strain and uniaxial stress on silica scale growth process were investigated and compared. For the case of constant strain load, the induced stress was relaxed gradually. While for the case of uniaxial stress load, the induced stress increased with oxidation time.
3. Generally, tensile stress or strain accelerated the oxidation diffusion process. However, under uniaxial stress, the reaction rate at the interface was retarded, which was not found in the case of constant strain load.

## ACKNOWLEDGMENTS

The authors are grateful for the support by National Natural Science Foundations of China (51175177, 51322510 and 51371082). The author Xian-Cheng Zhang is also grateful for the

support by Special Programs for Key Basic Research of Science and Technology Commission of Shanghai Municipality (13DJ1400202 and 12JC1403200).

[1] B. E. Deal and A. S. Grove, J. Appl. Phys. **36**, 3770 (1965).
[2] A. Kole and P. Chaudhuri, AIP Adv. **4**, 107106 (2014).
[3] L. Shen, Z. C. Liang, C. F. Liu, T. J. Long, and D. L. Wang, AIP Adv. **4**, 027127 (2014).
[4] K. Kimoto, H. Tanaka, D. Matsushita, K. Tatsumura, and S. Takeno, AIP Adv. **2**, 042144 (2012).
[5] M. A. U. Usman, B. J. Smith, J. B. Jackson, M. C. D. Long, and M. S. Miller, AIP Adv. **3**, 032112 (2013).
[6] L. M. Mack, A. Resiman, and P. K. Bhattacharya, J. Electrochem. Soc. **136**, 3433 (1989).
[7] D. B. Kao, J. P. Mcvittie, W. D. Nix, and K. C. Sarasat, IEEE Trans. Electron Devices **ED-34**, 1008 (1987).
[8] E. Kobeda and E. A. Irene, J. Vac. Sci. Technol. B **4**, 720 (1986).
[9] A. Szekeres and P. Danesh, Semicond. Sci. Technol. **11**, 1225 (1996).
[10] N. B. Pilling and R. E. Bedworth, J. Inst. Met. **29**, 529 (1923).
[11] B. Pieraggi and R. A. Rapp, Acta Metall. **36**, 1281 (1988).
[12] B. Pieraggi, R. A. Rapp, and J. P. Hirth, Oxid. Met. **44**, 63 (1994).
[13] V. K. Tolpygo, J. R. Drygen, and D. R. Clarke, Acta Mater. **46**, 927 (1998).
[14] D. R. Clarke, Acta Mater. **51**, 1393 (2003).
[15] S. Maharjan, X. C. Zhang, F. Z. Xuan, Z. D. Wang, and S. T. Tu, J. Appl. Phys. **110**, 063511 (2011).
[16] S. Maharjan, X. C. Zhang, and Z. D. Wang, J. Appl. Phys. **112**, 033514 (2012).
[17] S. Maharjan, X. C. Zhang, and Z. D. Wang, Oxid. Met. **77**, 93 (2012).
[18] Y. H. Suo and S. P. Shen, J. Appl. Phys. **114**, 164905 (2013).
[19] J. L. Ruan, Y. M. Pei, and D. N. Fang, Corros. Sci. **66**, 315 (2013).
[20] J. L. Ruan, Y. M. Pei, and D. N. Fang, Acta Mech. **223**, 2597 (2012).
[21] A. Fargeix and G. Ghibaudo, J. Appl. Phys. **56**, 589 (1984).
[22] A. Fargeix and G. Ghibaudo, J. Appl. Phys. **54**, 7153 (1983).
[23] M. Navi and Scott. T. Dunham, J. Electrochem. Soc. **144**, 367 (1997).
[24] H. Noma, H. Takahashi, H. Fujioka, M. Oshima, Y. Baba, K. Hirose, M. Niwa, K. Usuda, and Norio Hirashita, J. Appl. Phys. **90**, 5434 (2001).
[25] T. J. Delph and M. Lin, J. Mater. Res. **14**, 4508 (1999).
[26] E. A. Irene, E. Tierney, and J. Angilello, J. Electrochem. Soc. **129**, 2594 (1982).
[27] E. A. Irene, J. Appl. Phys. **54**, 5416 (1983).
[28] E. Kobeda and E. A. Irene, J. Vac. Sci. Technol. B **6**, 574 (1988).
[29] D. B. Kao, J. P. McVittie, W. D. Nix, and K. C. Saraswat, IEEE Trans. Electron Devices **ED-35**, 25 (1988).
[30] P. Sutardja and W. G. Oldham, IEEE Trans. Electron Devices **36**, 2415 (1989).
[31] T. Tamura, N. Tanaka, M. Tagawa, N. Ohmae, and M. Umeno, Jpn. J. Appl. Phys. **32**, 12 (1993).
[32] S. Alexandrova, A. Szekeres, and J. Koprinarova, Semicond. Sci. Technol. **4**, 876 (1989).
[33] J. Y. Yen and J. G. Hwu, Appl. Phys. Lett. **76**, 1834 (2000).
[34] J. Y. Yen and J. G. Hwu, J. Appl. Phys. **89**, 3027 (2001).
[35] A. Mihalyi, R. J. Jaccodine, and T. J. Delph, Appl. Phys. Lett. **74**, 1981 (1999).
[36] M. T. Lin, R. J. Jaccodine, and T. J. Delph, J. Mater. Res. **16**, 728 (2001).
[37] J. P. Hirth and W. A. Tiller, J. Appl. Phys. **56**, 947 (1984).
[38] W. A. Tiller, J. Electrochem. Soc. **127**, 625 (1980).
[39] A. M. Lin, R. W. Dutton, D. A. Antoniadis, and W. A. Tiller, J. Electrochem. Soc. **128**, 1121 (1981).
[40] H. S. Moon, Ph. D. Thesis, Seoul National University, Seoul, 2002.
[41] S. A. Schafer and S. A. Lyon, Appl Phys. Lett. **47**, 154 (1985).
[42] B. J. Mrstik, A. G. Revesz, M. Ancona, and H. L. Hughes, J. Electrochem. Soc. **134**, 2020 (1987).